KAM Tori Construction Algorithms

William E. Wiesel [1]

Air Force Institute of Technology
2950 Hobson Way,
Wright-Patterson AFB, OH 45433

Abstract

In this paper we evaluate and compare two algorithms for the calculation of KAM tori in Hamiltonian systems. The direct fitting of a torus Fourier series to a numerically integrated trajectory is the first method, while an accelerated finite Fourier transform is the second method. The finite Fourier transform, with Hanning window functions, is by far superior in both computational loading and numerical accuracy. Some thoughts on applications of KAM tori are offered.

1. Introduction

The KAM theorem has laid nearly unnoticed for almost sixty years. Named for Kolmogorov [4], Arnold [1], and Moser [8], this theorem predicts that most lightly perturbed Hamiltonian trajectories should lie on the surface of a torus. This is a multiply-periodic structure that should be represented as a Fourier series in multiple variables. What makes this different from a perturbation theory is that the Fourier series and its basis frequencies need not be approximate: they have definite values, to which a perturbation theory itself is only an approximation.

The potential applications of KAM tori are numerous. They should provide the general solution to the problem of formation flight in a Hamiltonian system. They can be used as another way to compress an ephemeris, and potentially can be used as the starting point for perturbations due to any remaining forces.

To achieve this promise, we must have an efficient way to produce a KAM torus passing through a given set of initial conditions, and assess its accuracy.

2. Two Algorithms

In this work we derive and compare the accuracy and performance of two numerical algorithms for constructing KAM tori. The first of these has already been mentioned in the literature, and consists of numerical fitting a KAM torus to the result of a numerical integration of an orbit. This seems to be the most direct method. Second, we consider extracting the Fourier coefficients of the torus from a numerically integrated Fourier transform.

Since the KAM theorem applies directly to Hamiltonian systems, it is only necessary to find the Fourier series for the system coordinates q_i. It is being assumed here that the system is posed in a set of "primitive" or "native" coordinates, so that the kinetic energy portion of the Hamiltonian is quadratic in either the generalized velocities $\dot{q}_i$, or equivalently the momenta p_i. This means that the kinematic half of Hamilton's equations, $\dot{q}_i = \partial\mathcal{H}/\partial p_i$ are a linear set of equations

$$\dot{\mathbf{q}} = A(q)\mathbf{p} + \mathbf{b}(q) \tag{1}$$

in the momenta $\mathbf{p}$, and can be directly solved to find

$$\mathbf{p} = A^{-1}\dot{\mathbf{q}} - A^{-1}\mathbf{b} \tag{2}$$

The particular forms of the matrix $A(q)$ and the vector $\mathbf{b}(q)$ depend on the actual Hamiltonian system. It is to be noted, however, that the time derivatives of the coordinates can be easily extracted from the same Fourier series that produce the coordinates, so that it is not necessary to carry separate series for the system momenta p_i.

[1] The views expressed are those of the author, and do not necessarily reflect those of the United States Air Force, the Department of Defense, or the U.S. Government.
email: William.Wiesel@afit.edu

Report Documentation Page

Form Approved
OMB No. 0704-0188

1. REPORT DATE	2. REPORT TYPE	3. DATES COVERED
SEP 2008		**00-00-2008 to 00-00-2008**

4. TITLE AND SUBTITLE	5a. CONTRACT NUMBER
KAM Tori Construction Algorithms	5b. GRANT NUMBER
	5c. PROGRAM ELEMENT NUMBER
6. AUTHOR(S)	5d. PROJECT NUMBER
	5e. TASK NUMBER
	5f. WORK UNIT NUMBER
7. PERFORMING ORGANIZATION NAME(S) AND ADDRESS(ES) **Air Force Institute of Technology,2950 Hobson Way,Wright-Patterson AFB,OH,45433**	8. PERFORMING ORGANIZATION REPORT NUMBER
9. SPONSORING/MONITORING AGENCY NAME(S) AND ADDRESS(ES)	10. SPONSOR/MONITOR'S ACRONYM(S)
	11. SPONSOR/MONITOR'S REPORT NUMBER(S)

12. DISTRIBUTION/AVAILABILITY STATEMENT
Approved for public release; distribution unlimited

13. SUPPLEMENTARY NOTES
2008 Advanced Maui Optical and Space Surveillance Technologies Conference, 16-19 Sep, Maui, HI.

14. ABSTRACT
In this paper we evaluate and compare two algorithms for the calculation of KAM tori in Hamiltonian systems. The direct fitting of a torus Fourier series to a numerically integrated trajectory is the first method, while an accelerated finite Fourier transform is the second method. The finite Fourier transform, with Hanning window functions, is by far superior in both computational loading and numerical accuracy. Some thoughts on applications of KAM tori are offered.

15. SUBJECT TERMS

16. SECURITY CLASSIFICATION OF:			17. LIMITATION OF ABSTRACT	18. NUMBER OF PAGES	19a. NAME OF RESPONSIBLE PERSON
a. REPORT	b. ABSTRACT	c. THIS PAGE			
unclassified	**unclassified**	**unclassified**	**Same as Report (SAR)**	**9**	

Also, we note that for multiply periodic functions $f(t) = f(\mathcal{Q} = \boldsymbol{\omega} t)$ that

$$\begin{aligned} ||f(t)|| &= \left\{ \frac{1}{(2\pi)^M} \int_0^{2\pi} f(\mathcal{Q})^2 d\mathcal{Q}_1 d\mathcal{Q}_2 ... d\mathcal{Q}_M \right\}^{1/2} \\ &= \left\{ C_0^2 + \frac{1}{2} \sum_{\mathbf{j}} \left(C_{\mathbf{j}}^2 + S_{\mathbf{j}}^2 \right) \right\}^{1/2} \end{aligned} \tag{3}$$

is a norm on the space of M dimensional multiply periodic functions. It satisfies all three properties required of a norm: it is zero if and only if $f \equiv 0$, $||kf(t)|| = k\,||f(t)||$ for scalar k, and $||f(t) + g(t)|| \leq ||f(t)|| + ||g(t)||$. The first two properties are trivial to show, while the last follows easily from the Fourier series form of the norm using the equivalent result for the Euclidean norm. Note that invoking the ergodic theorem, Arnold and Avez [2], the space integral form of the norm (3) can be evaluated as a time integral

$$||f(t)|| = \left\{ \lim_{T \to \infty} \frac{1}{T} \int_0^T f(t)^2 dt \right\}^{1/2} \tag{4}$$

for Hamiltonian systems. We will find this result useful in evaluating how successfully we have approximated KAM tori. One version of this is the norm of the error in the equations of motion

$$||\Delta \dot{p}|| = \left|\left| \dot{\mathbf{p}} + \frac{\partial \mathcal{H}}{\partial \mathbf{q}} \right|\right| \tag{5}$$

where the torus Fourier series supplies the coordinates and via (2) the momenta, and a time derivative of (2) gives the predicted $\dot{\mathbf{p}}$. This is averaged over the torus via (3).

Finally, the notation $\mathcal{Q} = \boldsymbol{\omega} t$ is to indicate that these variables are one realization of the Hamilton-Jacobi separation coordinates.

2.1 Direct Fitting of Trajectories

If a trajectory lies on a KAM torus, then the coordinates can be represented as a Fourier series. Since it seems the most obvious thing in the world to numerically integrate Hamilton's equations to produce a trajectory, fitting the result of such a numerical integration is the obvious first method. It has been done in [7], and also by the current author, [11].

Write the Fourier series representation of the KAM torus as

$$\mathbf{q}(t) = \mathbf{C_0} + \sum_{\mathbf{j}} \left\{ \mathbf{C_j} \cos(\mathbf{j} \cdot \boldsymbol{\omega} t) + \mathbf{S_j} \sin(\mathbf{j} \cdot \boldsymbol{\omega} t) \right\} \tag{6}$$

The multiple summation vector $\mathbf{j}^T = (j_1, j_2, ... j_N)$ is, of course, bounded above, and the KAM torus basis frequencies are most conveniently handled as a vector $\boldsymbol{\omega}^T = (\omega_1, \omega_2, ... \omega_N)$. The usual rules for the sine and cosine of a negative argument imply that the first nonzero index j_i should be positive to avoid duplicate terms in the series, and therefore singular least squares matrices. After the "first" positive index, subsequent indices are bounded between specified truncation limits $-j_{k,max} \leq j_k \leq j_{k,max}$. This makes for a somewhat cumbersome index summation coding, but is absolutely essential to obtain a nonsingular problem.

In the direct trajectory fitting method, (6) is the observable relation needed for least squares fitting. Its linearization is then easily found, the matrix

$$\mathcal{T} = \frac{\partial \mathbf{q}}{\partial \mathcal{X}} \tag{7}$$

where the unknowns are the Fourier coefficients $\mathbf{C_j}$, $\mathbf{S_j}$ as well as the system basis frequency set $\boldsymbol{\omega}_k$. The problem is nonlinear with the inclusion of the basis frequency set. This is perhaps the most general case, since each coordinate should have the same basis frequencies, and that forces the problem into the nonlinear regime. On the other hand, if the basis frequencies are determined separately in advance, see [5], [11], then each coordinate can be fit separately, and the algorithm becomes a linear least squares problem. We have

not adopted this option. The residuals $\mathbf{r}_i$ at the points from the numerical integration are then calculated, and corrections to the state are given by the usual least squares formula

$$\delta\mathcal{X} = \left(\mathcal{T}^T\mathcal{T}\right)^{-1}\mathcal{T}\mathbf{r} \tag{8}$$

Note that this requires the inversion of ever larger matrices as the order of the Fourier series is increased.

2.2 Finite Time Fourier Transforms

The usual definition of the Fourier transform of a function of time $f(t)$ is

$$\mathcal{F}(\nu) = \int_{-\infty}^{\infty} f(t)e^{-2\pi\nu it}dt \tag{9}$$

In any numerical application, of course, the use of infinite time intervals is out of the question, and the Fourier transform of a multiply periodic function becomes an inconvenient sum of delta functions, which are difficult to handle numerically. It then becomes natural to investigate the finite time Fourier transform

$$\begin{aligned}\mathcal{F}_T(\nu) &= \frac{1}{2T}\int_{-T}^{T} f(t)e^{-2\pi\nu it}\chi_p(t)dt \\ &= \frac{1}{2T}\int_{0}^{T} f(t)e^{-2\pi\nu it}\chi_p(t)dt - \frac{1}{2T}\int_{0}^{-T} f(t)e^{-2\pi\nu it}\chi_p(t)dt\end{aligned} \tag{10}$$

While the Fourier transform is defined in terms of the cycle frequency ν, we will most often cite results in terms of the angular frequency $\omega = 2\pi\nu$. In our application the functions $f(t)$ will be coordinates of a Hamiltonian system obtained by numerical integration of a trajectory. The symmetric time interval form of the Fourier transform requires two separate integration intervals when starting from a nominal $t = 0$. While this is somewhat of a complication, it does make best use of the finite accuracy available through a numerical integration, and there are other advantages as well.

Following Laskar [6] we have written $\chi_p(t)$ for a cosine window, or Hanning window function, where

$$\chi_p(t) = \frac{2^p(p!)^2}{(2p)!}\left(1 + \cos\left(\frac{\pi t}{T}\right)\right)^p \tag{11}$$

Laskar has studied the accelerated convergence of the frequency determination when a window function is used. We will see shortly that they are also extremely advantageous in decoupling spectral line amplitudes. We have found that it is very desirable to produce the numerical integration of the orbit $f(t)$ as a first step, and then to import it into the Fourier transform code as a very large vector $f(t_i)$. This allows efficient mechanization of (10) by, e.g. Simpson's rule, and also allows multiple analysis options without repeating the orbit integration.

Fig. 1 shows the Fourier transform of a single spectral line using the first four Hanning acceleration functions. The finite Fourier transform oscillates with a frequency of

$$\omega_T = \pi/T \tag{12}$$

so this plot shows only the immediate vicinity of the spectral line at ω_0. There are several things to note from this plot. First, the peak amplitude is unaltered by using different Hanning functions. Simple calculation gives the Fourier series coefficients for a single line as

$$C = 2\Re\mathcal{A}_0, \quad S = 2\Im\mathcal{A}_0 \tag{13}$$

where $\mathcal{A}_0$ is the peak amplitude. (The constant term can be found either as $C_0 = \Re\mathcal{A}(\omega = 0)$, or from the initial conditions.) Second, while it is well known that higher order Hanning functions accelerate the convergence properties of finding the peak frequency, they also broaden the peak. This expands the realm of convergence to the actual spectral line frequency ω_0 without confusion by sidelobes. Finally, recall that the entire spectrum will be an infinite summation of such spectral lines. We have found that without a Hanning function, the amplitude of one line $\mathcal{A}_0$ can be significantly changed by the far tails of adjacent lines. This

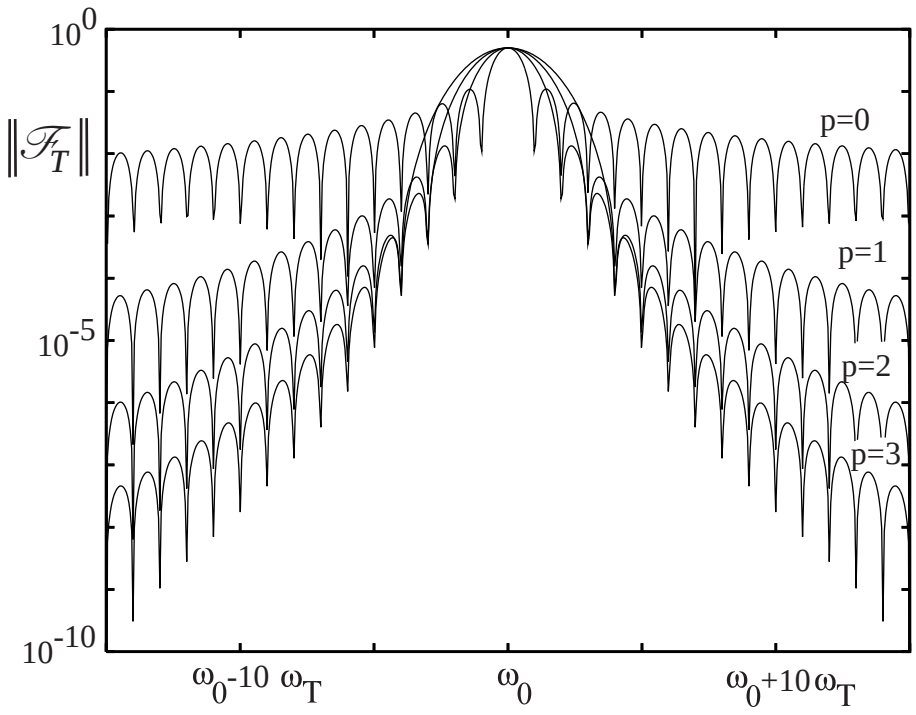

Figure 1: Fourier transform of a single spectral line with unit amplitude, using different Hanning functions.

makes it necessary to solve a large system of linear equations. On the other hand, by the time $p = 2$, which we now use for all cases, the sidelobes decay very, very quickly. This means that we can directly use (13) for all but the very closest adjacent lines. (Parenthetically, note that if two lines are very close, so that $\mathbf{j} \cdot \boldsymbol{\omega} \approx \mathbf{k} \cdot \boldsymbol{\omega}$, then

$$(\mathbf{j} - \mathbf{k}) \cdot \boldsymbol{\omega} \approx 0 \tag{14}$$

which is just another form of the resonance condition. So, if a KAM torus exists (no resonance), the above will not be a problem.) This is a huge advantage of the finite Fourier transform method, since the decoupling of spectral lines makes it possible to solve very large problems one spectral line at a time.

Finally another advantage of the finite Fourier transform method is that it does not require an approximation to the actual KAM Fourier series, as does the nonlinear trajectory fitting method. Rather, only an approximate knowledge of the system frequencies is needed.

3. Numerical Results

In this effort we have studied a series of tori in the restricted problem of three bodies, see e.g. [10]. The Hamiltonian function is given by

$$\mathcal{H} = \frac{1}{2}\left(p_x^2 + p_y^2\right) + yp_x - xp_y - \frac{1-\mu}{r_1} - \frac{\mu}{r_2} \tag{15}$$

in the usual rotating frame of reference. Here μ is the mass of the smaller primary, and the radii are given by

$$r_1^2 = (x-\mu)^2 + y^2, \quad r_2^2 = (x+1-\mu)^2 + y^2 \tag{16}$$

One advantage of studying this system is that we can use the surface of section technique to visualize the tori, [3], We have studied a group of tori for a value of $\mathcal{H} = -1.6$ with $\mu = 0.01214$, nearly the earth / moon ratio, and the usual dimensionless units being used. The periodic orbit at the core of the tori has initial conditions

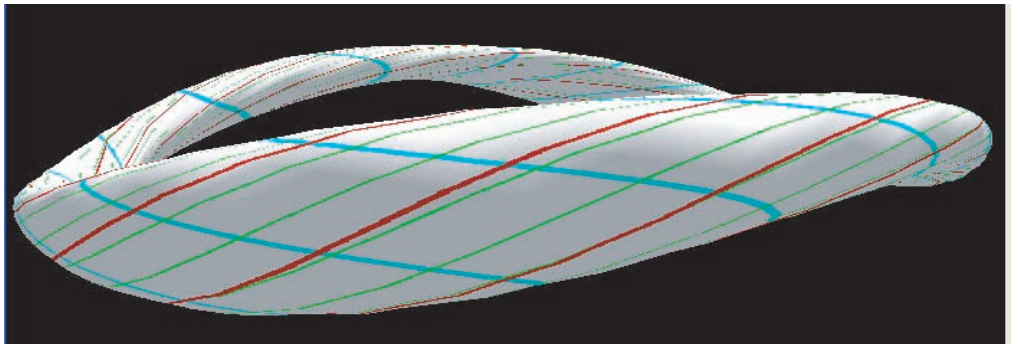

Figure 2: A three dimensional view of a KAM torus.

$x = 0.55954260514673$, $p_y = 1.4186361935797$ with $y = p_x = 0$, and a period of $\tau = 5.597166681940$ time units (TU). This gives the single torus frequency for the periodic orbit as $\omega_1 = 1.1225653378258$ radians per time unit. While the periodic orbit itself has only one frequency, nearby tori should approximate the Floquet solution, so the second frequency should be nearly the Poincaré exponent $\omega_P = 0.1592640457$ radians / TU for this orbit. Of course, the Fourier series for the periodic orbit can be obtained by standard numerical methods. Finally, we note that this group of tori is part of the 2:1 resonance structure for this mass value.

Most of the results that follow are for the torus that has initial conditions $x = 0.600$, $y = 0$, $p_x = 0$, $p_y = 1.3322289632022$. A view of the final constructed torus is shown in Fig. 2. Blue and green lines are lines of constant $\mathcal{Q}_1$ and $\mathcal{Q}_2$, while the trajectory is shown in red. While this can appear complicated when projected back into the physical phase space, the transformation actually makes the dynamics quite simple. All the $\mathcal{Q}_i$ coordinates are linear in time. Fig. 3 shows the behavior in the torus coordinate space. In fact, this is the "surface texture" used in the three dimensional model of Fig. 2

One point that needs to be brought out here is that all methods depend on knowing the torus frequencies with relatively good accuracy when beginning the fit, by any of the methods discussed. These use relatively large final times t_{max} for a numerical integration in order to sample the torus are required when attempting to sample uniformly across the $\mathcal{Q}$ space. While no numerical integration is required fitting the equations of motion. In order for the linearization we have used to be valid, this means that the error in the separation coordinates $\delta\mathcal{Q}_i \approx \delta\omega_i t_{max} << 1$. Since the final time may be relatively large, this implies that the frequency error must be correspondingly small when even beginning the process. The author suspects that fits that do not converge convincingly to small errors may have "hung" with an error in some phases $\delta\mathcal{Q}_i$ that is not small.

The question of how far to extend the Fourier solution naturally arises. Fig. 4 shows the result of fitting a restricted problem torus using the least squares process, and by the finite Fourier transform. The orbit fit solution uniformly improves until a limit is reached, beyond which improvement comes more slowly, if at all. This may be associated with the accuracy limits involved in the solution of a very large linear system of equations in the case of the least squares orbit fit. The finite Fourier transform results continue to improve for some considerable time after the orbit fitting process has reached an accuracy floor. Since the Fourier transform computational burden grows only linearly with the number of spectral lines included, it has a clear advantage here both in terms of accuracy and in terms of computational loading.

The residuals in the orbit points assumes an interesting form once the match between the torus and the numerical integration is close enough. When the two are still significantly apart, definite patterns appear in the residuals, and the power spectral density plot of the residuals will often reveal where significant structure is yet to be accounted for. But when close, the coordinate residuals often assume a form as shown in Fig 5. This linear trend can only be accounted for by an error in one or more fundamental torus frequencies. A missing harmonic would, of course, produce a periodic signature in the residuals. But an error in a frequency, if small enough, shows up as

$$S_k \sin((\omega_0 + \delta\omega)t) \quad = \quad S_k \sin(\omega_0 t)\cos(\delta\omega t) + S_k \cos(\omega_0 t)\sin(\delta\omega t)$$

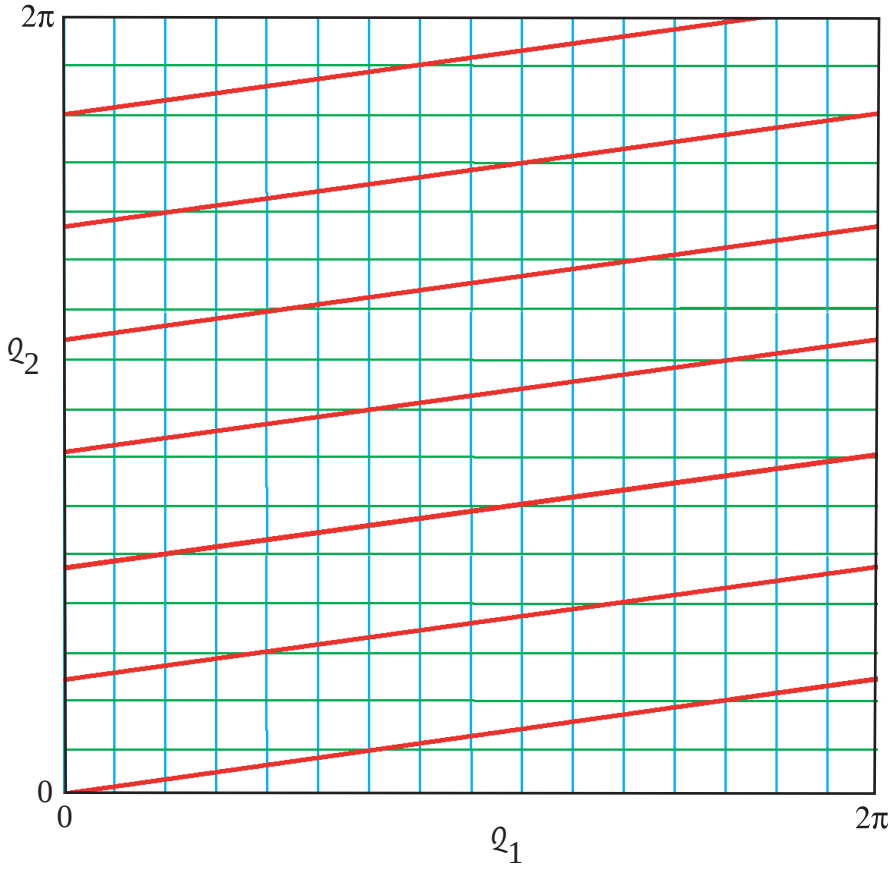

Figure 3: Motion on the torus surface is simple straight line motion.

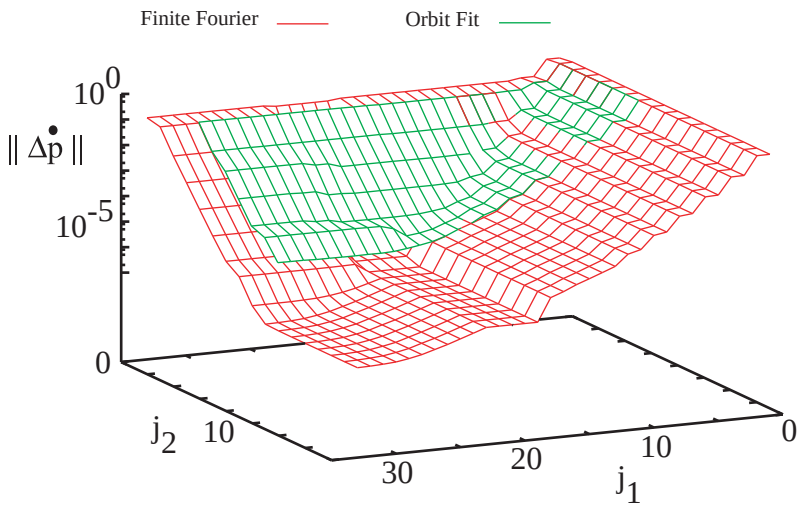

Figure 4: Equation of motion error norm for direct fitting of a torus from a numerical integration. Red is the Fourier transform, while Green shows the orbit fit results.

$$\approx \quad S_k \sin(\omega_0 t) + S_k \cos(\omega_0 t)\delta\omega t \tag{17}$$

This produces a secular term in the residuals. The error shown in Fig 5, which has a growth of a few parts in 10^6 over a time interval of several thousand time units implies an error in a frequency of a few parts in 10^9. This may be in the torus decomposition, or an error in the numerical integration. But it is a very small effect. And in fact, it may arise from the numerical integration, since the discrete jumps in the slope cannot come from the Fourier series.

4. Action Momenta

The Fourier series angles $\mathcal{Q}_i = \Omega_i t$ are the N separation coordinates expected from the Hamilton-Jacobi theorem. Their conjugate momenta are the action variables [9]

$$\mathcal{P}_i = \frac{1}{2\pi} \oint_{\Gamma_i} \mathbf{p} \cdot d\mathbf{q} \tag{18}$$

where the integral is carried out around the N irreducible contours Γ_i around the torus. This is easily done with the torus Fourier series in hand, since we integrate around one new coordinate $\mathcal{Q}_i$, holding all the others constant. It is also known that these integrals are invariant to the particular realization of these contours. Starting from the fitted Fourier series for the coordinate vector $\mathbf{q}$, the system momenta can be found through the kinematic half of Hamilton's equations, $\dot{\mathbf{q}} = \partial\mathcal{H}/\partial\mathbf{p}$. This often can be rearranged into the form

$$\mathbf{p} = T_2\dot{\mathbf{q}} + T_1\mathbf{q} \tag{19}$$

where the matrix T_2 comes from the quadratic part of the kinetic energy, and the matrix T_1 most often appears when a rotating reference frame is employed. Of course, this is not the most general form of the system momenta, but will be sufficient for this paper. Then the coordinate rates are obtained by a time derivative

$$\dot{\mathbf{q}} = \sum_{\mathbf{j}} (\mathbf{j} \cdot \boldsymbol{\omega}) \left\{ -\mathbf{C}_\mathbf{j} \sin(\mathbf{j} \cdot \vec{\theta}) + \mathbf{S}_\mathbf{j} \cos(\mathbf{j} \cdot \vec{\theta}) \right\} \tag{20}$$

where we have extended the scalar definition (6) to a vector of coordinates $\mathbf{q}$. Also, then, we can write the differential $d\mathbf{q}$ for contour Γ_i as

$$d\mathbf{q} \quad = \quad \frac{\partial \mathbf{q}}{\partial \theta_i} d\theta_i$$

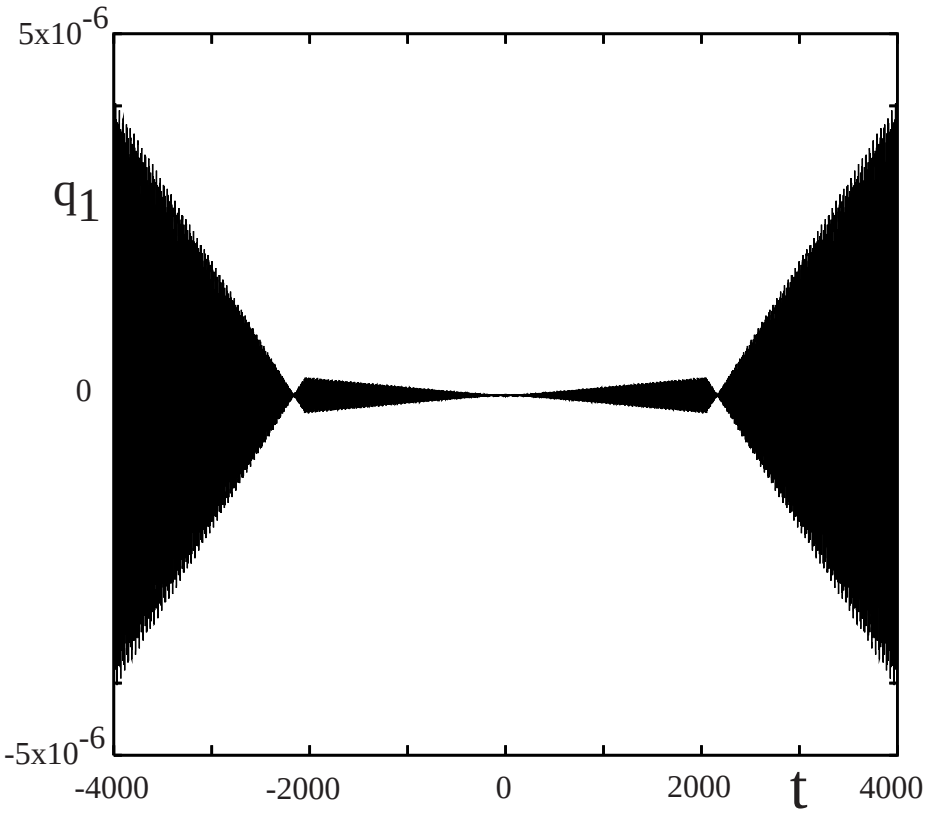

Figure 5: Coordinate residuals when the torus fitting error is dominated by a frequency error and frequency jumps.

$$= \sum_{\mathbf{j}} j_i \left\{ -\mathbf{C_j} \sin(\mathbf{j} \cdot \vec{\theta}) + \mathbf{S_j} \cos(\mathbf{j} \cdot \vec{\theta}) \right\} d\theta_i \tag{21}$$

So, having fit the KAM coordinates $\mathbf{q}$ and having obtained the basis frequencies Ω_i, it is then possible to numerically calculate the conjugate action momenta $\mathcal{P}_i$.

4. Conclusions and Prospectus

In this paper it has been shown that the finite Fourier transform algorithm has very great advantages in both accuracy and computational loading for reducing numerically integrated orbits to KAM Tori. This process has been carried out to better than single precision accuracy, and the resulting Fourier series allow the reduction of the dynamics to local Hamilton-Jacobi form: the coordinates increment linearly with time, while the momenta are constant.

Research currently is proceeding in applying KAM torus theory to earth satellites, including the problems of formation flight, stationkeeping satellite constellations, compressing ephemeris data for navigational satellites, and the important problem of determining a torus from observational tracking data. This latter problem involves the solution to the problem of motion in the vicinity of a KAM torus, which the author hopes to report on shortly.

References

[1] V. Arnold. Proof of kolmogorov's theorem on the preservation of quasi-periodic motions under small perturbations of the hamiltonian. *Rus. Math. Surv.*, 18(N6):9–36, 1963.

[2] V. I. Arnold and A. Avez. *Ergodic Problems in Classical Mechanics*. W. A. Benjamin, New York, N.Y., 1968.

[3] William H. Jefferys. An atlas of surfaces of section for the restricted problem of three bodies. *Applied Mechanics Research Laboratory*, AMRL 1034:1–20, 1971.

[4] A.N. Kolmogorov. On the conservation of conditionally periodic motions under small perturbations of the hamiltonian. *Dokl. Akad. Nauk. SSSR*, 98:469, January 1954.

[5] Jacques Laskar. Introduction to frequency map analysis. In C. Simo, editor, *Hamiltonian Systems with Three or More Degrees of Freedom*, pages 134–150, 1999.

[6] Jacques Laskar. Frequency map analysis and quasiperiodic decompositions. *Proceedings of Proquerolles School*, pages 1–31, Sept 2001.

[7] Colin McGill and James Binney. Torus construction in general gravitational potentials. *Mon. Not. R. Astron. Soc.*, 244:634–645, January 1990.

[8] J.K. Moser. On invariant curves of an area preserving mapping of an annulus. *Nachr. Akad. Wiss. Göttingen, Math. Phys.*, Kl. IIa:1–20, January 1962.

[9] Edward Ott. *Chaos in Dynamical Systems*. Cambridge University Press, Cambridge, UK, second edition, 2002.

[10] V. Szebehely. *Theory of Orbits*. Academic Press, New York, N.Y., 1967.

[11] W. E. Wiesel. Earth satellite orbits as kam tori. *Journal of the Astronautical Sciences*, (to appear):AAS 07–423, July 2007.